Article

pubs.acs.org/Biomac

Surface and Tribological Behaviors of the Bioinspired Polydopamine Thin Films under Dry and Wet Conditions

Wei Zhang,[†,∥] Fut K. Yang,[†,∥] Yougun Han,[†,∥] Ravi Gaikwad,[‡] Zoya Leonenko,[‡,§,∥] and Boxin Zhao*[,†,∥]

[†]Department of Chemical Engineering, [‡]Department of Physics, [§]Department of Biology, and [∥]Waterloo Institute for Nanotechnology, University of Waterloo, 200 University Avenue West, Waterloo, Ontario, Canada N2L 3G1

ABSTRACT: Dopamine is a "sticky" biomolecule containing the typical functional groups of mussel adhesive proteins. It can self-polymerize into a nanoscale thin film on various surfaces. We investigated the surface, adhesion, friction, and cracking properties of polydopamine (PDA) thin films for their effective transfer to functional devices and biocompatible coatings. A series of surface characterizations and mechanical tests were performed to reveal the static and dynamic properties of PDA films coated on glass, polydimethylsiloxane (PDMS), and epoxy. We found that PDA films are highly hydrated under wet conditions because of their porous membrane-like nanostructures and hydrophilic functional groups. Upon dehydration, the films form cracks when they are coated on soft substrates due to internal stresses and the large mismatch in elastic modulus. The adhesive pull-off force or the effective work of adhesion increased with the contact time, suggesting dynamic interactions at the interface. A significant decrease in friction forces in water was observed on all three material surfaces coated with PDA; thus, the film might serve as a water-based lubrication coating. We attributed the different behavior of PDA films in air and in water to its hydration effects. These research findings provide insight into the stability, mechanical, and adhesive properties of the PDA films, which are critical for their applications.

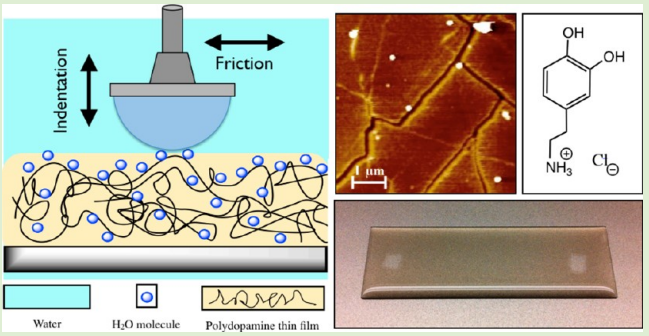

1. INTRODUCTION

With the rapidly growing demand to miniaturize the devices in biomedical-, electronic-, or energy-related industries, thin film technologies have been developed and extensively used in the application of such advanced functional materials as semiconductors, biosensors, corrosion resistant coatings, and medical polymers.[1,2] Compared with bulk materials, thin films are almost 2-D and have a larger surface-to-volume ratio, which make them more sensitive to surface properties and interactions.[3] There is a large number of coating strategies that can deposit thin films with precisely controlled thickness and functionality; they include plasma deposition, layer-by-layer deposition, the deposition of Langmuir−Blodgett films, monolayer self-assembly, and the emerging polydopamine (PDA) coating.[4−8] Among these techniques, the PDA coating has been demonstrated as a possible "versatile" and "multifunctional" coating and functionalization method.[9] To effectively transfer the PDA coating into engineering application, the stability, mechanical, and adhesion properties of the coating films are almost equally important as the function of the thin film itself. We report an experimental study of the surface and material properties of the PDA thin films deposited on different substrates both in air and in water.

Inspired by the chemistry of the adhesive plaques of marine mussels, dopamine, a biological neurotransmitter, has been found to have a remarkable capability to adhere and self-polymerize to form a nanoscale PDA film on support surfaces.[9−11] Dopamine, with the chemical structure of catecholamine, can be regarded as a small-molecule mimic of the adhesive component, L-DOPA, of marine mussels.[12,13] On the basis of the assumption that the coexistence of the amine and catechol groups is important for achieving underwater adhesion, dopamine has been proposed and demonstrated by Lee et al. as a multifunctional coating for various substrates, including both inorganic and organic materials (Figure 1a).[9,14] Since then, we have seen an increasing interest in the exploration of PDA film in a range of applications, including the conventional surface and material engineering and the emerging of bio- and nanotechnology.[15,16] Nevertheless, the most fundamental aspect of PDA thin film, its structure, is still under debut at present. The well-accepted dopamine polymerization mechanism is shown in Figure 1b (route 1),[17] where catechol can be oxidized to a quinone, followed by its structural rearrangement and polymerization; an alternative approach for PDA formation involves the supramolecular aggregation achieved through charge transfer, π-stacking, and hydrogen-bonding interactions (Figure 1b, route 2).[18]

Because PDA films contain a high density of functional groups (amino and catechol) on the surface, it can be used to immobilize, regulate, and sense biomolecules, for example, cells, proteins, and amino acids. There is a large number of studies of the surface modification with PDA on various substrates for

Received: October 10, 2012
Revised: January 4, 2013
Published: January 11, 2013

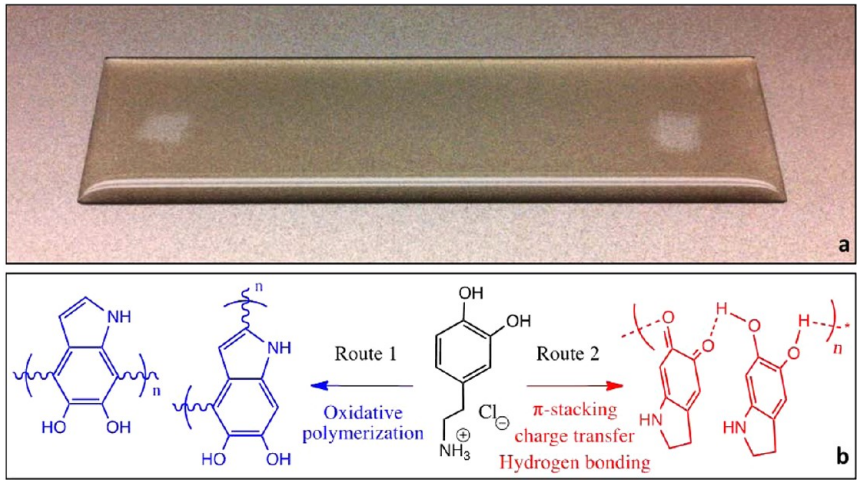

Figure 1. (a) Digital photo of an apparently homogeneous PDA-coated PDMS surface. (b) Two plausible mechanisms of dopamine self-polymerization proposed in literature.[17,18]

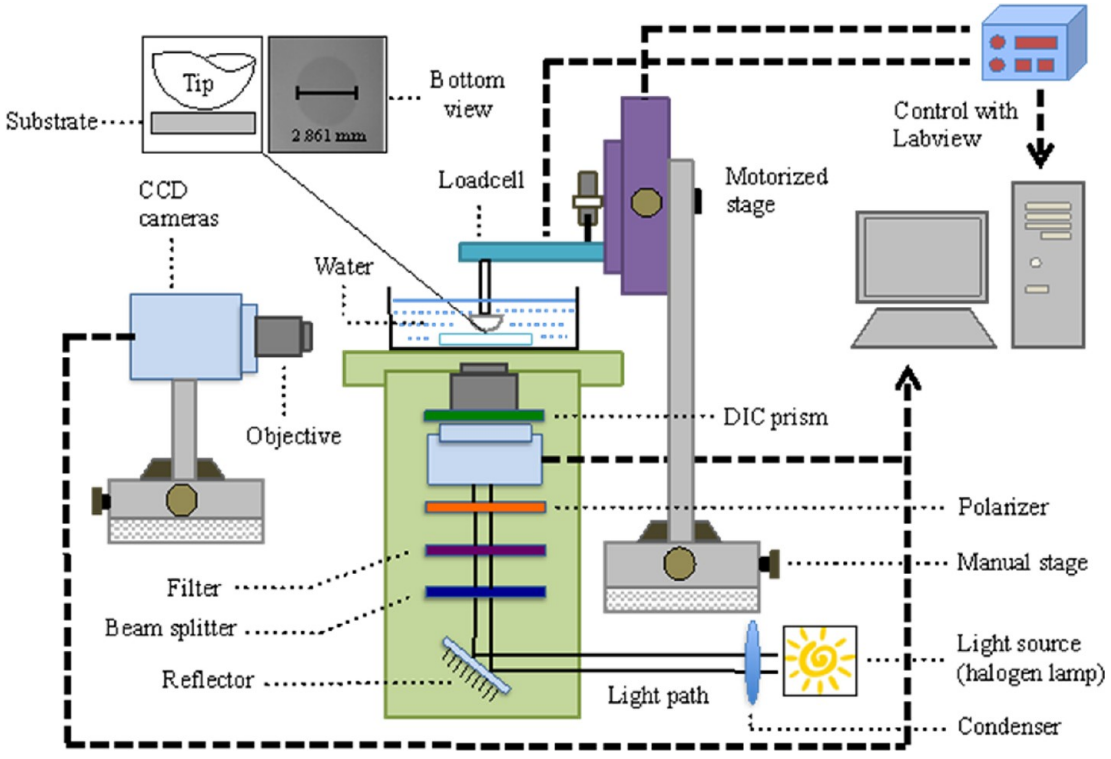

Figure 2. Schematic of the microindentation apparatus consisting of a hemispherical elastomer probe attached to a load cell and displacement controllers (a nanopositioner and motorized linear stage), a sample stage (with a water bath) attached on an inverted optical microscope, a standalone side-view camera, and a LabVIEW controlling program with a computer and monitor.

bioengineering, including biomolecule grafting,[19] cell adhesion,[17] biomineralization,[20] and drug encapsulation.[21] These studies have provided strong evidence of the use of PDA films as a promising way to optimize material surface chemistry. In contrast, the mechanical and adhesion properties of the PDA film are still largely unexplored, even though its importance in the application of PDA films has been realized.[15,22] A typical study in this aspect is the contact angle-measurement of PDA films, which reveals its hydrophilic nature and the associated surface energy as estimated to be 40 mJ/m^2.[23] The effect of coating temperature and dopamine concentration on hydrophobic polymers were also investigated, showing that the PDA films became thicker with higher coating temperature and dopamine concentration.[24] Our previous research focused on studying the adhesive properties of the PDA coating with contact adhesion, and adhesive bonding tests.[23,25] However, these PDA thin film investigations so far only concerned the film itself instead of the influence of the substrates. Furthermore, most of those studies focused on PDA under dry conditions, and there is a need to measure the mechanical and adhesion properties of PDA thin film under wet conditions because it was frequently used for bioengineering where water is the media.[26,27] From our studies and other recent reports in literature, we hypothesize that the material properties of hydrated PDA films are significantly different from those of

dx.doi.org/10.1021/bm3015768 | Biomacromolecules 2013, 14, 394−405

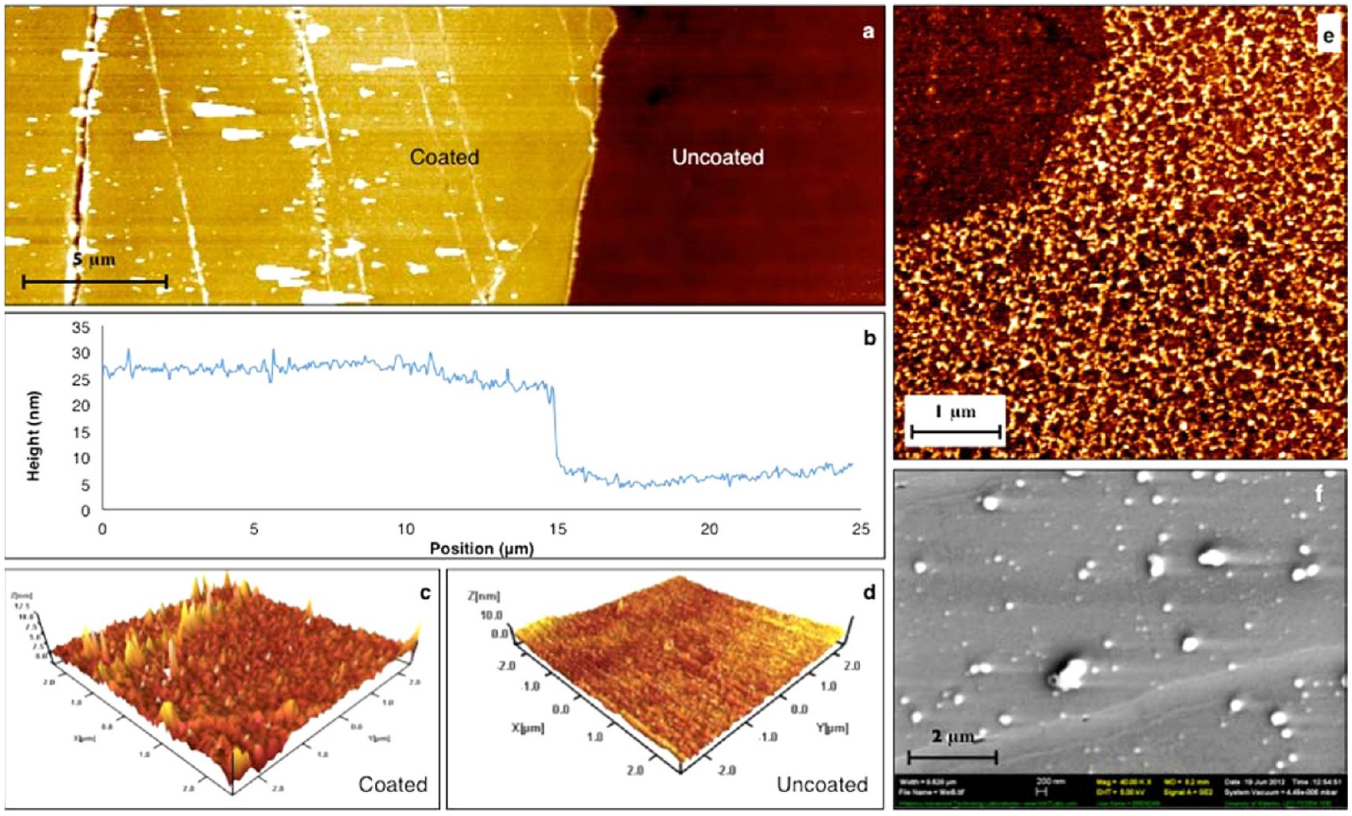

Figure 3. Surface characterizations of polydopamine thin films: (a) a typical AFM topography image of PDA-coated and uncoated PDMS substrate; (b) cross-section plot from the AFM image showing the thickness of the PDA film deposited on PDMS substrate; (c) 3-D AFM image of PDA coated PMDS; (d) 3-D AFM image of uncoated PDMS; (e) AFM topography image of PDA-coated glass surfaces showing the nanoporous structures of PDA film (the dark area at the left top corner is partially coated surface); and (f) SEM image of PDA coated PDMS surface, showing the microsized PDA particles.

dehydrated ones, affecting the mechanical stability and functionalities of PDA films.

The objective of this study is to investigate the mechanical stability and durability of PDA films, which are essential to the success of their applications. A series of experimental studies were carried out to characterize the PDA thin film coated on three typical well-defined substrates, glass, polydimethylsiloxane (PDMS), and epoxy to investigate the material behaviors of PDA film under a mechanical stress/strain field and the effects of coating substrates. Microindentation measurements combined with Johnson−Kendall−Roberts (JKR) contact mechanics theory[28] were used to systematically study the tribological properties (i.e., adhesion, friction, and wears) of the PDA thin films under both dry conditions and under water. We found that the fundamental properties of PDA under water are not equal compared with those exhibited under dry conditions, revealing a significant hydration effect on the surface chemistry and qualities of the coatings.

2. EXPERIMENTAL SECTION

2.1. Materials. PDMS (Sylgard 184 elastomer kit, Dow Corning) solution was prepared by mixing the elastomer base and cross-linker at a weight ratio of 10:1. The flat sheet of PDMS was made by casting 2 mL of PDMS solution onto a microscope slide and curing at 90 °C for 1.5 h in ambient air. Epoxy (322, Dow Corning) solution, used for making elastomers, was prepared by mixing the elastomer base and cross-linker at a weight ratio of 100:13. The flat sheet of epoxy was made by casting 2 mL of epoxy solution onto a microscope slide and curing at 70 °C for 10 min and 130 °C for 1 h in ambient air. The hemispherical tip of PDMS was made by first molding the PDMS solution into a hemispherical shape using a custom-made Teflon mold and then coating the resulting PDMS tip with a layer of PDMS solution to make the tip surface smooth. The tip core was cured at 90 °C for 15 min, and the tip coating along with the core was then cured at 90 °C for 1.5 h. The radii of the tips are ∼2.9 mm, varying slightly from batch to batch; the exact values were determined by analyzing the side-view images for each indentation test.

The coating of PDA thin films on glass, PDMS, and epoxy substrates was performed inside a Petri dish by immersing the substrates in a dilute aqueous solution of dopamine hydrochloride (Fisher BioReagents), buffered to pH 8.5 (2 mg of dopamine per mL of 10 mM tris). To minimize the deposition of PDA micro/nanoaggregates formed during the coating process, all samples were placed upside down in the buffer solution. After 24 h of coating, the samples were rinsed with ultrapure water and dried in air or stored in ultrapure water.

To estimate the water contents of PDA, the PDA nanoparticles were synthesized via the oxidation of dopamine solution (2 mg of dopamine per milliliter of 10 mM tris) by atmospheric oxygen in an open vessel at room temperature for 24 h. The black nanoparticles were collected from the solution by centrifugation (8000 rpm) for 15 min, then washed with ultrapure water three times and stored in ultrapure water.

2.2. Methods. The surface characteristics of the PDA thin film were examined by optical microscope (Carl Zeiss Axio Observer. Z1m), scanning electron microscope (SEM; Zeiss LEO 1550), and two types of atomic force microscopy (NanoWizard II AFM, JPK Instruments AG, Berlin; and Dimension 3100 AFM, Veeco Metrology Group). The adhesion and friction tests were performed on a custom-made microindentation apparatus, as illustrated in Figure 2. A hemispherical PDMS tip or probe was mounted on a load cell (Transducer Techniques TMO-2) that was attached to a compact

dx.doi.org/10.1021/bm3015768 | Biomacromolecules 2013, 14, 394−405

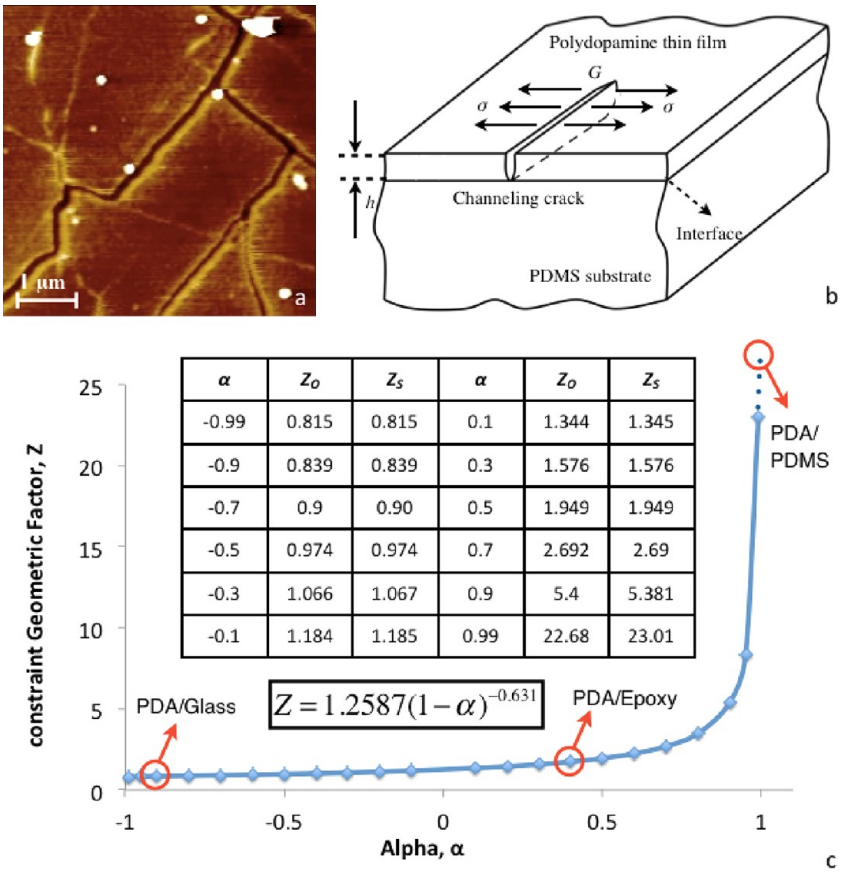

Figure 4. Cracking of dehydrated PDA films on PDMS surface: (a) AFM image of PDA thin film cracks on PDMS substrate; (b) illustration of a channel crack in PDA thin film on PDMS substrate; and (c) values of function $Z(\alpha)$ with respect to the parameters α and the comparison with Beuth's original data.[34]

nanopositioner (PI P-611. XZS) with a resolution of 0.2 nm and a 100 μm travel distance. The nanopositioner was fixed on a movable linear stage (Newport ESP-MFA-CC) with a range of 25 mm. The movement of the PDMS tip was controlled by the nanopositioner and a displacement controller (PI E-625. PZT). An inverted optical microscope (Carl Zeiss Axio Observer. Z1m) equipped with a CCD camera (Carl Zeiss Axio Cam 1Cm1) was adopted to monitor the area of the contact spot and its deformations. The load, displacement, contact area, and time were recorded by a custom-written LabVIEW program.

Microindentation measurements of the PDMS tip on glass, PDMS, and epoxy substrates were performed at room temperature. In each experiment, a tip was brought into contact with a flat substrate at 0.1 μm/sec until reaching a preload of 5 mN, then held in contact for 120 s, and at last separated at the same speed. The bottom view of contact spot between a probe and a substrate was recorded during the test. The associated force and contact radius were analyzed in the framework of JKR contact mechanics. For friction tests, a PDMS probe was brought into contact with a substrate until a normal force of 0.1g, 0.5g, 1g, or 2g was reached. Then, three cyclic reciprocating lateral movements of the substrate were carried out with a sliding speed of 30 μm/s while keeping the normal force constant using a force-controlling feedback system. During underwater experiments for both indentation and friction tests, stronger light source, polarizer, and image filter were utilized to obtain high-quality images of the contact spots. Both tips and substrates were immersed in water for 0.5 h before testing.

For contact-angle measurements, a syringe pump was used to inject and withdraw water or diiodomethane at a constant rate of 100 μL/min on PDA-coated epoxy substrates. Advancing and receding angles were measured by expanding the volume of a 5 μL water or diiodomethane droplet and subsequently withdrawing the droplet. The images of the drop were recorded and analyzed by a custom-developed LabVIEW program. All measurements were performed in ambient air at room temperature.

For gravimetric experiments, three types of PDA nanoparticles were prepared: (1) the hydrated PDA nanoparticles prepared by blotting the "free water" from the wet fresh powder with a piece of filter paper; (2) partially hydrated PDA prepared by evaporating the "surface water" from the first sample in 95% humility chamber for 2 days, and (3) dehydrated PDA prepared by air drying the wet fresh PDA powder at room temperature for 5 days. The weight of each sample was measured by an analytic balance with four decimal unit accuracy (i.e., 0.1 mg). Three replicas of gravimetric experiments were performed.

3. RESULTS AND DISCUSSION

3.1. Surface Characterizations of Polydopamine Thin Films. The surface qualities of PDA thin films coated on the glass, epoxy, and PDMS substrates were characterized by optical microscopy, SEM, and AFM. The optical images of the PDA deposited on glass and epoxy surfaces under dry and wet conditions showed a smooth and homogeneous surface. In contrast, numerous microsized cracks were present in the PDA film deposited on PDMS surface after dehydration, whereas no cracks were found when the film was stored in water. The thickness and surface roughness of the PDA thin films were determined by AFM, as shown in Figure 3a−d. The thickness of PDA thin films deposited on glass, PDMS, and epoxy substrate was found to be 12.4 ± 0.9, 16.5 ± 1.1, and 15.5 ± 0.5 nm, respectively. The root-mean-square (rms) surface roughness was measured for both uncoated substrate and PDA-coated surface of the three substrates to be 7.4 ± 0.2 and 15.5

dx.doi.org/10.1021/bm3015768 | Biomacromolecules 2013, 14, 394−405

± 0.4 nm for glass, 3.8 ± 0.8 and 9.0 ± 2.5 nm for PDMS, and 2.3 ± 0.4 and 8.4 ± 0.8 nm for epoxy. These data reveal that the PDA films on the two polymer substrates are thicker and smoother than that on the glass. Figure 3e is a high-resolution AFM image of PDA thin film coated on glass, showing its noncontinuous membrane-like porous structure at the nanoscales. This porous structure may have contributed to the relatively high measured roughness, compared with the film thickness. The SEM image for PDA on PDMS substrate is shown in Figure 3f, revealing some deposited PDA particles whose size ranged from 50 to 80 nm. Such nanoparticles were also observed by Jiang et al[24] and Wei et al.[29] It is likely that the deposition of PDA nanoparticles on the PDA film was inevitable during the polymerization process. The PDA nanoparticles on the substrates may increase the heterogeneity and roughness of the surface, which may further influence the adhesion and friction properties of the film.[30,31] In this work, we examined the nature of this self-polymerized PDA coating as its own, instead of the ideal (smooth and homogeneous) PDA surface.

We further investigated the cracks on the PDA thin film coated on PDMS under dry conditions. Estimated from the AFM topographic images (a typical AFM image is shown in Figure 4a), the cracks were ∼50 nm in width and 15 nm in depth. The cracking of the PDA films has also been reported on silicon oxide substrate and poly(L-lactide) fiber surface under dry conditions by other researchers.[32,33] In the following, we applied the channel cracking model[34] to explain the cracking mechanism of PDA thin films on PDMS substrates under dry conditions.

For a thin elastic film bonded to a thick elastic substrate (Figure 4b), the driving force for the growth of cracks is defined as an energy release rate, as expressed in eq 1:

$$G = Z\frac{\pi}{2}\frac{\sigma^2 h}{E^*} \tag{1}$$

where σ, h, and E^* represent the residual stress, film thickness, and plane-strain elastic modulus, respectively. In the case of PDA film, the residual stress comes from the dehydration process during drying. The crack geometric factor Z depends on the elastic mismatch between the film and the substrate and the precise geometry.[35] Beuth calculated Z as a function of the two Dundurs parameters α and β for most practical material combinations and for the plane geometry:[36] The parameter α characterizes the elasticity mismatch between the film and the substrate as defined in eq 2; its numerical value ranges from −1 (which corresponds to an elastic film on a rigid substrate) to 1 (which corresponds to a rigid film on an elastic substrate). The parameter β is determined by the shear modulus and the Poisson's ratios of both the film and substrate; its value is well-approximated by $\alpha/4$.[37]

$$\alpha = \frac{E_f^* - E_s^*}{E_f^* + E_s^*} \tag{2}$$

In Beuth's original publication, he rigorously calculated $Z(\alpha, \beta)$ values as a function of α (the effect of β on the results is minor and can be neglected), as shown in Figure 4c. It is noted that Z does not change significantly when α is negative but increases rapidly when $\alpha > 0$, especially in the range from 0.5 to 1. On the basis of these data, we simplified the relationship between Z and α and fit it into a power-law function (eq 3) and plotted in Figure 4c. This power-law fitting curve overlaps with the Beuth's original plot.

$$Z = 1.2587(1 - \alpha)^{-0.631} \tag{3}$$

For comparison, Beuth's original Z_O value and the Z_S value formulated from our simplified Equation are listed in the insert table of the Figure 4c, and they are almost identical. In the following, we used eqs 1−3 and the previously determined elastic modulus and surface energy of PDA to obtain insight into the cracking phenomena of PDA films.

In our previous study, we determined $\alpha \approx -0.8$ for PDA-coated glass and $\alpha \approx 0.999$ for PDA-coated PDMS.[25] Similarly, for PDA-coated epoxy (E_s^* = 4.57 GPa),[38] the elasticity mismatching parameter α is determined to be 0.4. The Z values were calculated using eq 3, as shown in Figure 4c: Z = 0.87 for PDA-glass, Z = 1.74 for PDA-epoxy, and Z = 98.38 for PDA-PDMS. Assuming that the residual stress left after drying on the three different substrates is the same, the fact that no cracks formed on PDA-glass and PDA-epoxy suggests that their Z values are not high enough to generate a channel crack. In contrast, the Z value for PDA-PDMS is high enough to drive a channel crack at the same stress. Tentatively, we further the analysis to estimate the residual stress σ during the drying of PDA film by taking the minimum value for the G, that is, the work of cohesion of PDA film, that is $G = W_C = 2\gamma$ (where γ = 40 mJ/m^2).[23] In this way, the residual stress can be calculated from eq 1 to be 176 MPa. Note that the real residual stress should be far above this value because G is often higher than the work of cohesion.

3.2. Adhesion and Contact Deformations of the Polydopamine Thin Films Coating. The work of adhesion is a key thermodynamic parameter for characterizing the interactions between two dissimilar surfaces. We employed two methods (thermodynamic calculation and microindentation measurements) to determine the work of adhesion of PDA films and the probe PDMS surface in air and in water; our purpose is to elucidate the effect of water on the adhesive properties of PDA films. Preliminary tests showed the hydrophobic PDMS tips displayed a moderate adhesion to the substrates, allowing for the examination of the effect of PDA coating films.

The Owens−Wendt method was applied to estimate the work of adhesion from the surface energy components of the contacting surfaces.[39] For two surfaces α and β contacting in air (A), assuming air behaves like vacuum, the work of adhesion (W) can be calculated by eq 4:[40]

$$W_{\alpha A\beta} = \gamma_\alpha + \gamma_\beta - \gamma_{\alpha\beta} = 2\left(\sqrt{\gamma_\alpha^d \gamma_\beta^d} + \sqrt{\gamma_\alpha^p \gamma_\beta^p}\right) \tag{4}$$

whereas the work of adhesion (W) between the α and β in water (H) is determined as[40]

$$\begin{aligned} W_{\alpha H\beta} &= \gamma_{\alpha H} + \gamma_{\beta H} - \gamma_{\alpha\beta} \\ &= 2\left(\gamma_H^d + \gamma_H^p + \sqrt{\gamma_\alpha^d \gamma_\beta^d} + \sqrt{\gamma_\alpha^p \gamma_\beta^p} - \sqrt{\gamma_\alpha^d \gamma_H^d} \right. \\ &\quad \left. - \sqrt{\gamma_\alpha^p \gamma_H^p} - \sqrt{\gamma_\beta^d \gamma_H^d} - \sqrt{\gamma_\beta^p \gamma_H^p}\right) \end{aligned} \tag{5}$$

The surface energy data from the literature are given in Table 1;[11,23,25,40,41] and the calculated works of adhesion between polymer PDMS and different substrates with/without PDA thin film coating both in air and in water are summarized in Table 2. For uncoated substrates, water increased the work of adhesion

Table 1. Dispersion (or Nonpolar) and Polar Components of Different Solid/Liquid Surface Energy

γ (mJ/m^2)	γ (mJ/m^2)	γ^d (mJ/m^2)	γ^p (mJ/m^2)
water[40]	72.2	21.2	51
PDMS-184[25]	18.0	18.0	0
epoxy[11]	46.2	41.2	5
glass[41]	69.79	24.79	45
polydopamine[23]	40	30	10

for PDMS and epoxy and decreased for glass, whereas the works of adhesions for PDA-coated three substrates in both air and in water are identical because the PDA films were assumed to mask the chemical nature of the substrates. These thermodynamic works of adhesion are used in the following as theoretical values to compare with the experimentally determined results.

The adhesion contact behaviors of PDA films were investigated by microindentation (Figure 2) during the compressive loading and the unloading processes. We employed this technique to examine the dynamic adhesive properties of the PDA coating on glass, PDMS, and epoxy substrates both in air and in water. Figure 5 showed the plots of the compressive force versus displacement during the loading, contact/holding, and unloading processes of the measurements on the PDA-coated epoxy surfaces at different contact times (a) in air and (b) under water. For all experiments carried out under dry conditions, the surface force induced a "jump-in" mechanical instability when the surfaces are close enough, whereas in water, this phenomenon was not observed because the surface forces are much smaller than those under dry conditions. The shape of the "loading" curve did not change, whereas the shape of the "unloading curve" changed significantly with contact time, where the pull-off force increased with time.

We analyzed this data set in the framework of JKR contact mechanics.[28] When a hemispherical probe with radius R and elastic modulus E_1 is brought into contact with a flat surface with elastic modulus E_2, the work of adhesion (W) and the combined elastic modulus (K) are related to the applied load (F) and the radius of the contact area (a) by eq 6:

$$a^3 = \frac{R}{K}[F + 3\pi RW + \sqrt{6\pi RWF + (3\pi RW)^2}\,] \quad (6)$$

Figure 6 plots the typical cubic contact radius versus force curve for the contact adhesion between two surfaces (PDMS tip on PDA-epoxy substrates both in air and in water). During the JKR experiments, a and R values were obtained by analyzing contact deformation of the bottom view and tip image of the side view, respectively, F was recorded by the LabVIEW program, and the work of adhesion (W) and elastic modulus

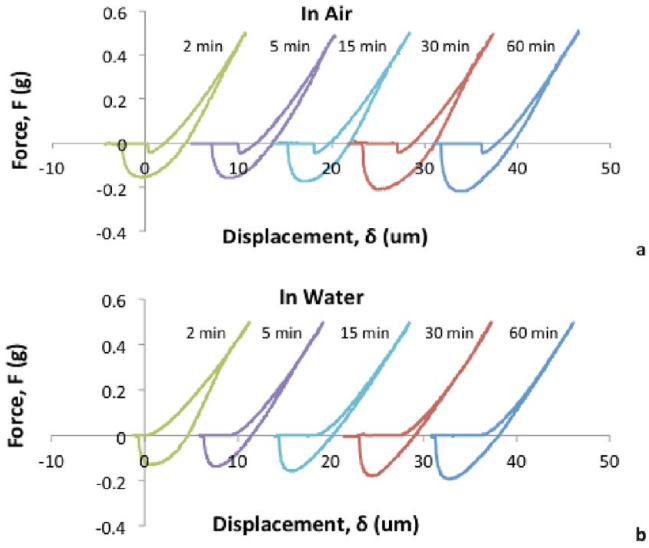

Figure 5. Typical plots of the compressive force versus displacement during the loading, contact/holding and unloading processes of the microindentation measurements on the PDA-coated epoxy surfaces at varied contact time (a) in air and (b) in water.

(K) were two fitting parameters estimated by the loading curve using the JKR model and the work of adhesion was summarized in Table 2. Under dry conditions, the works of adhesion determined by the microindentation are in the same order of magnitude as those thermodynamic ones determined by the Owens–Wendt method. Although the three substrates have varied surface energy and have different work of adhesion with the PDMS probe, the adhesion properties of their coated surfaces are almost identical, indicating that the nanoscale PDA film masked the surface chemistry of the substrates. In contrast, the measured works of adhesion by indentation test were significantly different from the calculated thermodynamic work of adhesion under wet conditions other than the one for bare glass surface. The measured works of adhesion on the three PDA coated surfaces were similar, but they were lower by more than one order of magnitude than those under dry conditions, reflecting the detrimental effects of water on adhesion. It should be noted that although cracks were found on dry PDA-PDMS substrate, during the microindentation process, there was no film delamination. Also, the area of the cracks was approximated to be only ~0.1% within the contact area, and thus the cracks have a negligible effect on the interactions between the tip and the PDA coating.

As shown in Figure 5, the loading curves and the unloading curves were not reversible; that is, there was a significant amount of loading–unloading hysteresis. This hysteresis

Table 2. Works of Adhesion between a PDMS Tip and Three Different Substrates (Bare and PDA-Coated) in Air and in Water

	thermodynamic work of adhesion		measured work of adhesion		effective work of adhesion (120 s holding time)	
work of adhesion (mJ/m^2)	in air	in H_2O	in air	in H_2O	in air	in H_2O
PDMS	36.00	102.36	35.5 ± 1.9	19.5 ± 2.8	67.3 ± 5.1	113.5 ± 4.7
PDA-PDMS	46.46	56.14	36.1 ± 1.1	2.4 ± 0.9	92.6 ± 21.1	46.4 ± 11.7
glass	42.24	5.92	41.3 ± 1.8	3.6 ± 0.8	119.1 ± 20.2	68.5 ± 17.9
PDA-glass	46.46	56.14	37.5 ± 2.2	4.8 ± 1.8	104.2 ± 7.3	95.7 ± 6.1
epoxy	54.46	68.57	40.9 ± 2.1	14.8 ± 0.9	116.9 ± 16.4	164.8 ± 13.1
PDA-epoxy	46.46	56.14	39.8 ± 2.5	2.1 ± 0.1	112.1 ± 18.1	79.4 ± 11.2

dx.doi.org/10.1021/bm3015768 | Biomacromolecules 2013, 14, 394–405

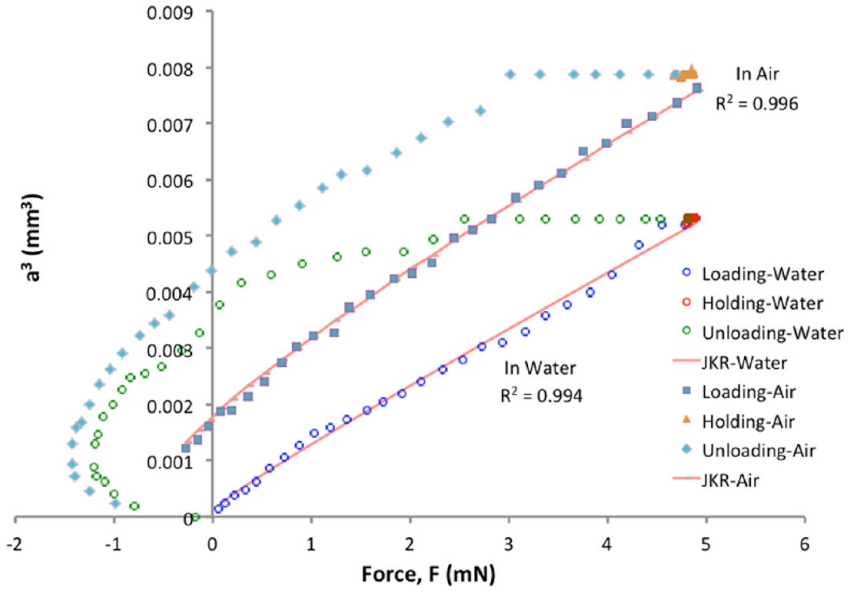

Figure 6. Plot of the cubic contact radius versus the compressive force during the loading, contact/holding, and unloading processes of the microindentation measurements on the PDA-coated epoxy surfaces in air and water. The solid lines are the JKR fitting curves to the loading process.

indicates time- and load-dependent interactions occurred between the PDA films and the PDMS probe surfaces, which consumed extra energy other than the thermodynamic free energy, as predicted by the JKR theory. It is useful to characterize the effective adhesion energy using the adhesive tensile force or pull-off force at the separation. This characterization might provide insight into the dynamic adhesion interactions of the PDA films. To perform further analysis, we extracted the pull-off force from Figure 5 and converted it into the effective work of adhesion W_{eff} using eq 7.

$$F_{\text{pull-off}} = \frac{3}{2}\pi R W_{\text{eff}} \tag{7}$$

The effective works of adhesion with 120 s contact/holding time were listed in Table 2, which are much larger than the works of adhesion measured in the loading curve. Figure 7 plotted the effective work of adhesion as a function of the contact time. We found that the effective work of adhesion calculated from unloading is significantly higher than what is measured during loading process, and it increased nearly linearly with contact time both in air and in water; this is reasonable considering the hysteresis effect and energy dissipation during the JKR loading−unloading cycle.[42,43] Also, the trends of changes in the effective work of adhesion with respect to the PDA coating are similar to those of the thermodynamic and measured work of adhesion.

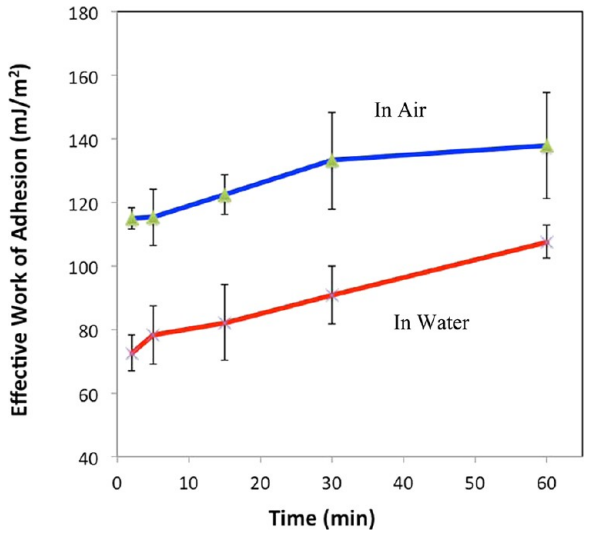

Figure 7. Effective works of adhesion $W_{eff} = 2F_{\text{Pull-off}}/3\pi R$ as a function of the contacting time for the microindentation tests on PDA-coated epoxy surfaces in air and in water.

3.3. Friction Behaviors of the Polydopamine Thin Films Coated on Different Substrates. Along with the adhesion properties, friction properties of a thin film are major concerns in the applications of thin films where both the normal loading force and the lateral shearing force are involved. The lateral force may damage the coating or even delaminate the film from its substrate. To the best of the authors' knowledge, there is no systematic study of the friction properties of PDA thin films. The lateral motion and force sensing components of the microindentation apparatus allowed us to investigate friction properties of the PDA films coated on the three substrates at varied preloads. Figure 8 shows the friction traces in terms of the lateral forces as a function of displacement for the PDMS tip on PDA-PDMS (Figure 8a) and PDA-epoxy (Figure 8b) substrates at 0.5 g indentation force in water. The average frictional force decreased with the number of cycles on the PDA-PDMS substrate. This suggests that the sliding motion damages the PDA film coated on the PDMS substrate. We did not see the decrease in the friction force for those coated on the epoxy and the glass substrates.

Figure 8c shows the contact spots obtained from the tests. The contact spot changed during the sliding process irrespective to the type of substrates: in air, the initially circular contact spot was deformed into a gibbous moon shape; and the contact area was smaller compared to the initial state. The sliding caused the PDA film coated on PDMS to crack and delaminate in the region ahead of the contact spot; for the films coated on glass and epoxy surfaces, there were no visible cracks. In general, the degree of damage was more pronounced in air

dx.doi.org/10.1021/bm3015768 | Biomacromolecules 2013, 14, 394−405

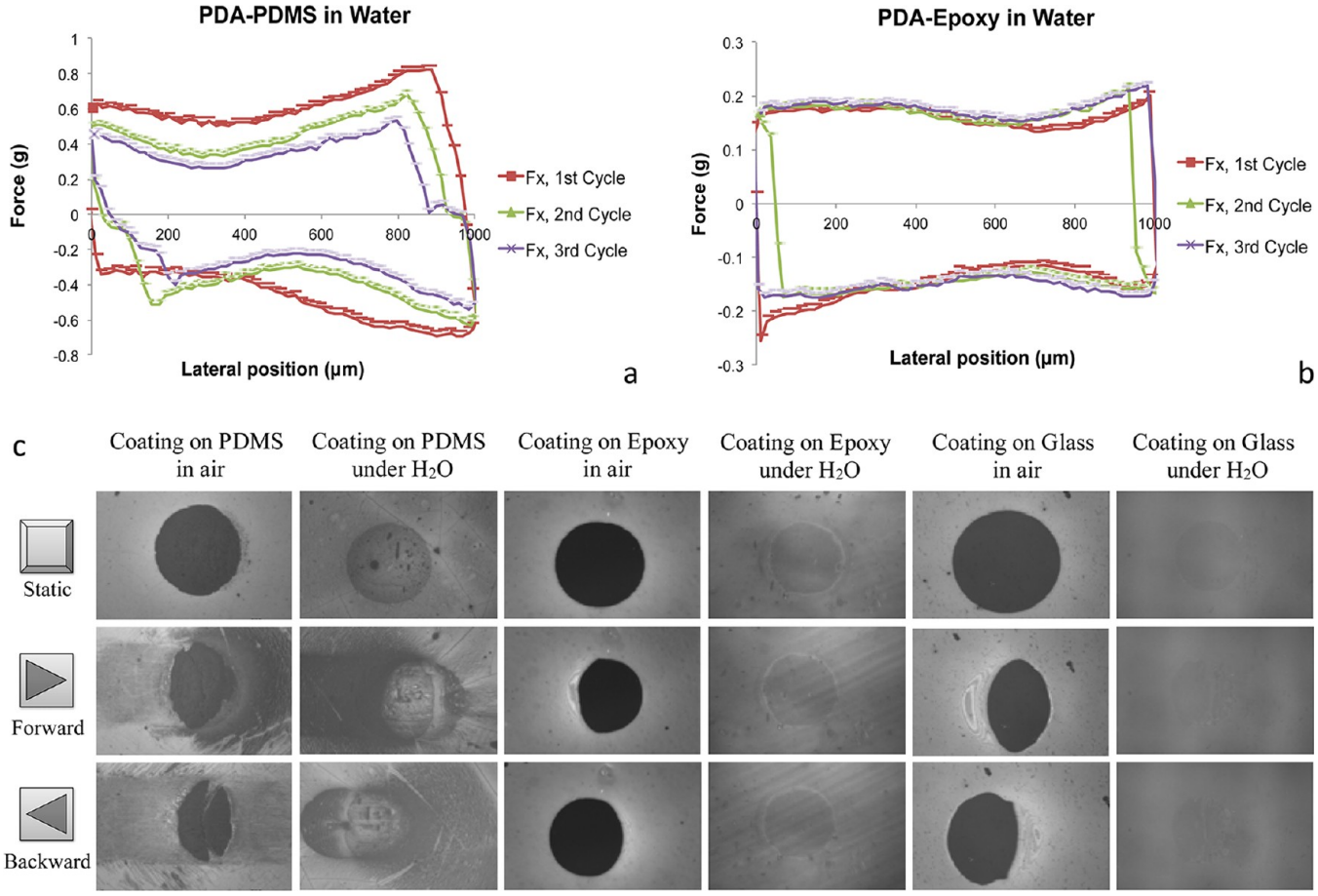

Figure 8. Plots of friction force versus lateral displacement during three cycles of reciprocating friction tests of (a) PDA coated PDMS surfaces in water; (b) PDA coated epoxy in water; and (c) optical images of PDA coated surfaces under dry and wet conditions during reciprocating friction tests including the initial contact (top panels), the forward sliding (middle panels), and the subsequent backward sliding (bottom panels).

than in water on PDMS surfaces, and no significant signs of crack or delimitation of the film were detected from the epoxy and glass surfaces.

Figure 9 shows the relationship between the load and the friction forces under different circumstances. The friction force F_f was calculated by averaging the values of lateral forces during sliding. It is generally proportional to the load with a finite intercept at zero preload. We applied the classical Amontons' law (eq 8) to these data sets, and the friction coefficient (μ_A) between a PDMS tip and PDA-coated/uncoated three substrates under dry and wet conditions at different loading forces was calculated and summarized in Table 3.

$$F_f = \mu_A F_N \tag{8}$$

The Amontons-type coefficient of friction μ_A at the low preload 0.1 g is significantly larger than those at high preloads, indicating the influence of molecular adhesion on friction. A careful examination reveals that PDA coating significantly reduced μ_A in water for all circumstances but increased μ_A for most situations in air other than the glass surface with 1 g preload.

In addition to the Amontons' Law, the Bowden and Tabor theory (eq 9), which added the adhesion component "σA" to eq 8, was found to fit the friction behavior of smooth surfaces, where the molecular adhesion effect is pronounced.[44,45]

$$F_f = \mu_B F_N + \sigma A \tag{9}$$

It should be noted that the coefficient μ_A in eq 8 is not the same as μ_B in eq 9. μ_A can be determined by Amontons' Law on each force point in Figure 9 and they may vary at different loads, while μ_B is identified as the slope of each line and preload independent. It appears that the eq 9 is more applicable to the friction behavior of the PDA films, suggesting the nanoscale porous structures of PDA films have not significantly limited the effect of molecular adhesion. However, eq 9 is only suitable for the surfaces that are undamaged during sliding, which means the PDA coated PDMS substrates in air need to be excluded from this system as a large amount of cracks were formed during friction process.

In the framework of Bowden and Tabor theory, eq 9, a detailed examination of the friction behaviors of PDA films was performed, and the fiction coefficient (μ_B) and adhesion component (σA) were calculated and summarized in Table 4. For PDA-coated glass and epoxy substrates, water changed both the slope or the fiction coefficient (μ_B) and the intercept or the adhesion component (σA); whereas in terms of uncoated surfaces, water influenced the intercept (σA) more significantly than the slope (μ_B) for all three substrates. Compared with dry conditions, σA was found to be smaller in water, which indicates that water may deteriorate the adhesion. Moreover, the PDA coating increased μ_B in air and decreased them in water for both glass and epoxy substrates, which are also consistent with the effect that PDA coating brought to μ_A (friction coefficient from Amontons' Law) at different

dx.doi.org/10.1021/bm3015768 | Biomacromolecules 2013, 14, 394−405

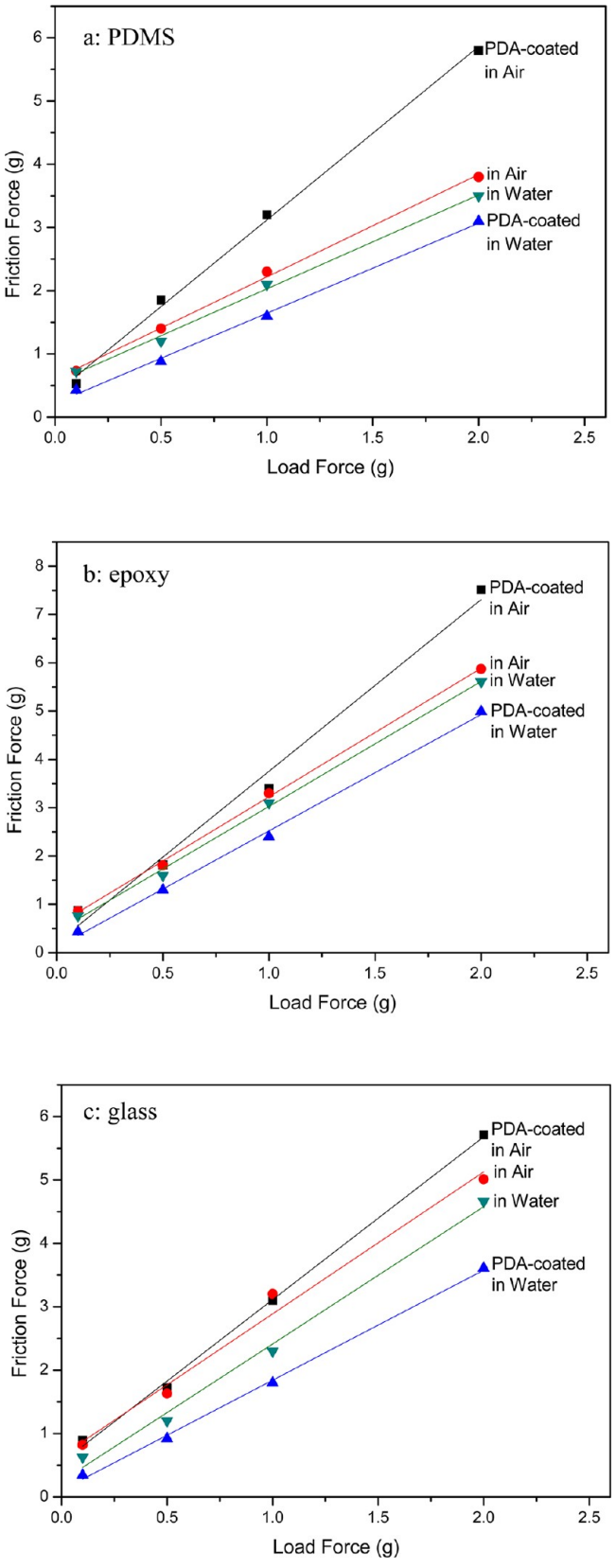

Figure 9. (a) Plots of loading forces versus friction forces on bare PDMS in air and in water and PDA-coated PDMS in air and in water. (b) Plots of loading forces versus friction forces on bare epoxy in air and in water and PDA-coated epoxy in air and in water. (c) Plots of loading forces versus friction forces on bare glass in air and in water and PDA-coated glass in air and in water.

indentation forces. It is also interesting to note that although eq 9 was not applicable to PDA-coated PDMS, the frictional data plotted in Figure 9a fell into a similar trend as the other two substrates. Overall, the lower friction forces and friction coefficients after PDA coating for all three substrates in water suggest that the PDA thin films might function as a lubricant in aqueous environment. It is interesting to notice that the self-polymerized dopamine is not a good adhesive in water, although the dopamine is a "sticky" biomolecule containing the typical functional groups of mussel adhesive proteins.

3.4. Hydration of Polydopamine Thin Films. The lubrication function of PDA coating in water indicated that the PDA films might be highly hydrated. A direct comparison of the behavior of PDA films under dry condition and under water supports this indication. First, there is no crack observed in PDA film in water, whereas numerous microsized cracks occurred on the PDA-coated PDMS because of the residual stress due to dehydration. Second, the work of adhesion measured by microindentation under dry condition is similar to the corresponding thermodynamic work of adhesion. In contrast, the measured work of adhesion by indentation test under wet condition was lower by one order of magnitude than the calculated thermodynamic work of adhesion (Table 2). A possible explanation for this is that the water molecules may have penetrated or diffused into the PDA film so as to alter its surface chemistry, which was not taken into account in the thermodynamic calculation.

The recent water contact angle studies of PDA film coated on PDMS conducted by Yang. et al revealed the possible formation of a hydration layer on PDA film.[23] Herein, we performed water contact angle experiments on PDA-epoxy to further verify the hydration effect of PDA films. Figure 10a,b presented the typical optical water drop images of growing and receding processes during the measurement. The advancing contact angle is 46°, and the receding contact angle is ~5°. Thus, the contact angle hysteresis, $\theta_a - \theta_r$ was determined to be ~40°. After the water drop completely withdrawn, there was a thin water layer left on the PDA surface (Figure 10c,d). For comparison, it is noted that the contact angle hysteresis on PDA-coated PDMS substrate was recorded at 60°.[23] Other than the different values of contact angles, both of these studies showed a large hysteresis, a small receding contact angle, and a significant pinning effect of the contact line; all of these phenomena confirmed the suspected hydration or other water–PDA interactions. However, it is likely that surface roughness posed by the PDA nanoparticles may contribute to the large contact angle hysteresis on PDA-coated PDMS and epoxy substrates. To address this concern, we performed diiodomethane contact angle measurement on the PDA-epoxy surface; diiodomenthane is a nonpolar organic liquid and is not able to hydrate the PDA surface. The diiodomethane's contact angle hysteresis on the PDA surface has been measured to be just 7° (Figure 10e,f), and there was no diiodomethane trace left on the PDA-epoxy surface after withdrawing the liquid (Figure 10g,h). The result suggests that whereas the roughness may affect the contact angle hysteresis, in the light of the significantly higher water contact angle hysteresis of 40°, we may conclude that the effect of roughness is minor and the hydration of the PDA thin films is the dominant factor for water contact angle hysteresis.

From this study and recent literature, it seems there might be three types of hydration effects, as illustrated in Figure 11. First, at the surface, PDA contains many hydroxyl groups, which

dx.doi.org/10.1021/bm3015768 | Biomacromolecules 2013, 14, 394–405

Table 3. Friction Coefficient (μ_A) between a PDMS Tip and Three Different Substrates (Bare and PDA-Coated) in Air and in Water at Four Different Indentation Forces

	0.1 g		0.5 g		1 g		2 g	
friction coefficient (μ_A)	air	H_2O	air	H_2O	air	H_2O	air	H_2O
PDMS	5.31	7.26	2.80	2.40	2.30	2.10	1.90	1.75
PDA-PDMS	7.30	4.28	3.70	1.96	3.20	1.60	2.90	1.55
glass	8.20	6.29	3.26	2.40	3.20	2.30	2.56	2.33
PDA-glass	8.93	3.44	3.44	1.84	3.10	1.80	2.86	1.81
epoxy	8.65	7.66	3.62	3.20	3.30	3.10	2.94	2.81
PDA-epoxy	8.71	4.33	3.64	2.60	3.40	2.40	3.76	2.55

Table 4. Adhesion Component (σA) and Friction Coefficient (μ_B) between a PDMS Tip and Three Different Substrates (Bare and PDA-Coated) in Air and in Water

	σA (in air)	σA (in water)	μ_B (in air)	μ_B (in water)
PDMS	0.6	0.55	1.62	1.48
PDA-PDMS	0.38	0.22	2.74	1.42
glass	0.65	0.25	2.24	2.16
PDA-glass	0.54	0.11	2.57	1.73
epoxy	0.57	0.44	2.66	2.59
PDA-epoxy	0.2	0.11	3.55	2.41

would attract water molecules to the surface and form hydrogen bonds with water molecules.[25,46] Second, some water molecules may be trapped into PDA film during the polymerization.[47] Third, PDA film has a porous membrane-like structure, the water molecules can penetrate or diffuse into these nanopores and they hydrate the free functional groups inside the films.[47,48] All of these actions may significantly reduce the rigidity of the PDA films and make it more durable under a mechanical stress field. Note that the second and third hydration actions occur inside the PDA film, and it is almost impossible to distinguish them experimentally. Thus, to a first approximation, we may say that there are two types of water associated with hydrated PDA:

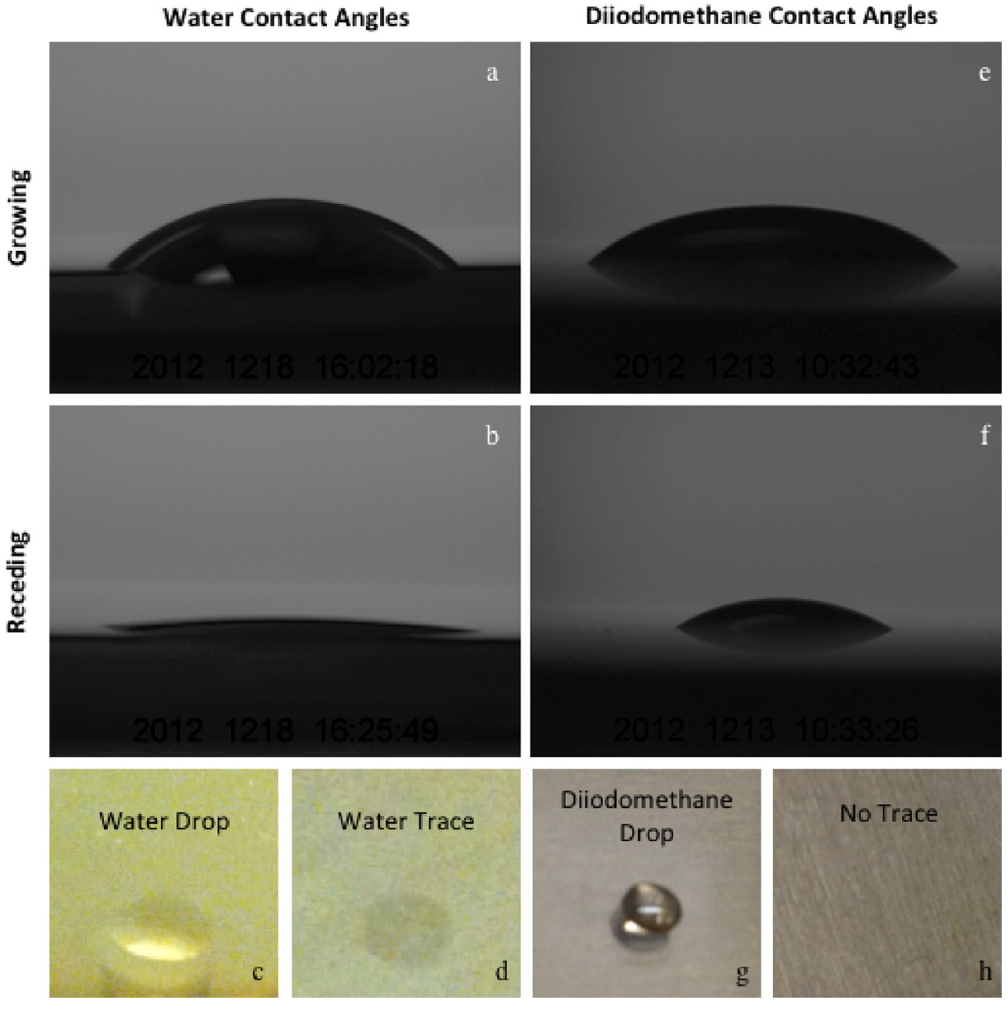

Figure 10. (a) Typical optical images of water contact angle at growing state; (b) typical optical images of water contact angle at receding state; (c) typical optical images of diiodomethane contact angle at growing state; (d) typical optical images of diiodomethane contact angle at receding state; (e) water drop on PDA coating; (f) water trace on PDA coating. (g) diiodomethane drop on PDA coating; and (h) no trace on PDA coating.

dx.doi.org/10.1021/bm3015768 | Biomacromolecules 2013, 14, 394−405

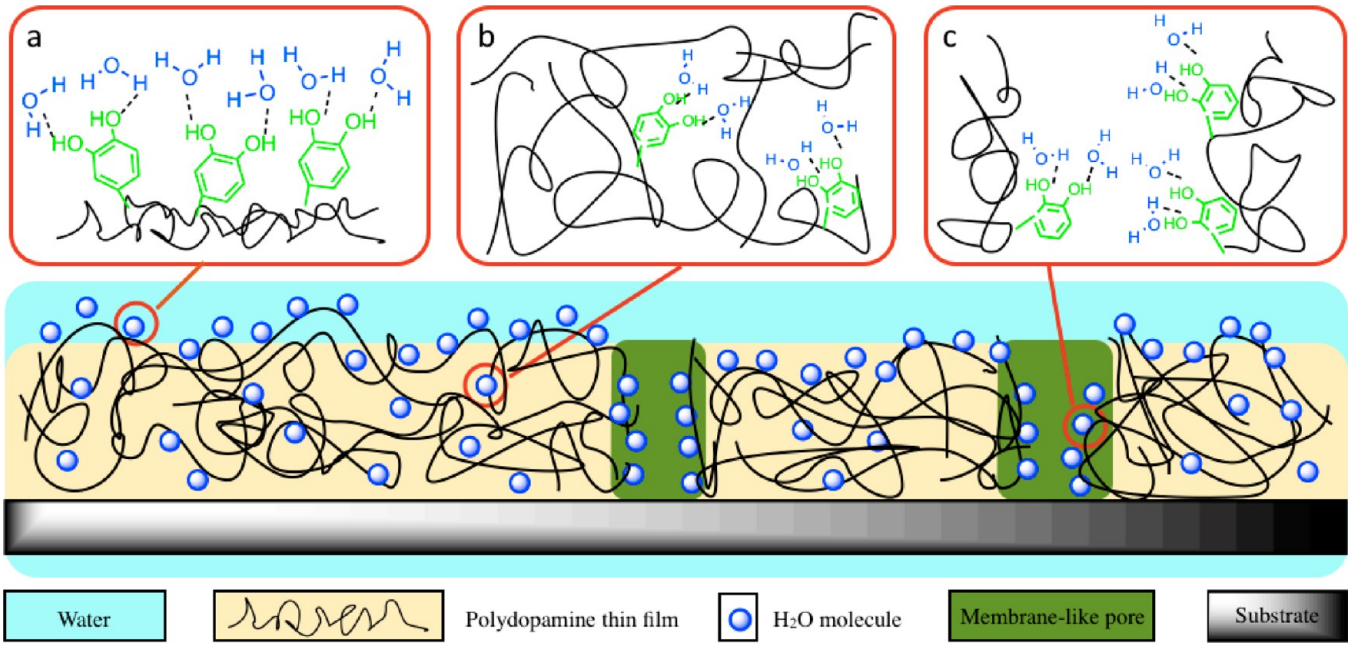

Figure 11. Illustrations of the hydration of polydopamine thin films: (a) surface hydration, (b) bulk hydration, and (c) diffusion of water into the nanopores of polydopamine films.

free water and trapped or bonded water. It will be informative to determine the relative amount of these two types of water to further elucidate the hydration effects. For this, we assumed that the PDA film and nanoparticles have the same hydration behaviors because they formed simultaneously during the self-polymerization of dopamine. The classical gravimetric measurements were performed with collected PDA nanoparticles. Three samples were prepared, and their weights were measured: (1) the hydrated PDA nanoparticles, (2) partially hydrated PDA nanoparticles, and (3) dehydrated PDA nanoparticles. The mass difference between the first and second sample was attributed to the "surface water", which was determined to be 248 ± 40% of the partially hydrated PDA nanoparticles weight. The mass difference between the second and third samples was attributed to the "bonded or trapped water", which was determined to be 86 ± 5%. To elucidate fully the hydration effects and their technical implications, a high precision microbalance may be required to perform the gravimetric measurement directly on the PDA nanoscale films. We also need to know the chemical structure of PDA, which is still not clear in literature at the moment. However, we may get indirect information from its analogue eumelanin. Eumelanin is a biological complex responsible for the pigmentation of skin, hair, and eye in human, whose mechanical, electrical and optical properties are strongly dependent on its hydration state.[47] On the basis of the high similarities of these two compounds, it is reasonable to expect that the hydration of the PDA has significant effects on the mechanical and chemical properties of the PDA thin films.

4. CONCLUSIONS

We investigated the surface and material properties of PDA films in terms of their morphology and adhesion, friction, wear, and cracking properties under both dry and wet conditions. The effects of substrates, on which PDA was deposited, were also investigated. The surface properties were examined by optical microscopy, AFM, and SEM, showing a porous membrane-like structure of the PDA films. Microsized cracks were found on the PDA deposited on PDMS dry surface, which is imposed by the mismatch of elastic modulus between the rigid film and its soft substrate. Microindentation techniques in combination with thermodynamic calculations and JKR contact mechanics analyses were employed to study the tribological behaviors – adhesion in normal direction and friction in lateral direction – of PDA films under both dry and aqueous conditions. The measured work of adhesion during loading in air between the PDMS tip and PDA-coated substrates is close to that of thermodynamic work of adhesion calculated; those underwater were much lower than that of the calculated thermodynamic work of adhesion. The adhesive pull-off force or the effective work of adhesion increased with the contact time, suggesting dynamic interactions at the interface. Friction properties of the PDA coating were characterized by both the friction forces and the coefficients of friction. A significant decrease in friction forces in water was observed on all three material surfaces coated with PDA, indicating the PDA coating might serve as a water-based lubrication coating. These research findings revealed a strong hydration effect of the PDA coating under wet conditions, which may be responsible for the observed different adhesion and friction properties in air and in water.

Finally, it might be useful to summarize the technical implications of these research findings on PDA films for their effective transfer into practical engineering application. First of all, the hydrated PDA films are more durable than dry films. Dehydration should be avoided because it may make the PDA film crack and then lose its integrity when coated on a soft substrate. If dehydration has to be involved, then it would be more appropriate to integrate PDA coating with rigid substrates, like epoxy or glass. Second, the effective works of adhesion between PDA films and the contacting probe are lower in water than in air; both of them increase with time, indicating dynamic interfacial interactions. These dynamic phenomena and the effect of medium should be considered

dx.doi.org/10.1021/bm3015768 | Biomacromolecules 2013, 14, 394–405

when using PDA films as an ad-layer to bond dissimilar materials. Finally, it is interesting to notice that the PDA coating reduced the friction coefficient of all three materials under water. In this regard, combined with the hydrophilic and biocompatible nature of the PDA molecule, the PDA coating may potentially function as a water-based lubricant for tissue engineering, for example, to reduce the contact stresses and protect the biomaterials from wear and damage.

AUTHOR INFORMATION

Corresponding Author

*E-mail: zhaob@uwaterloo.ca.

Notes

The authors declare no competing financial interest.

ACKNOWLEDGMENTS

This research was supported by a Discovery Grant from Natural Sciences and Engineering Research Council of Canada (NSERC) awarded to B.Z. We are grateful to Dr. Jian Zhang for help with part of AFM imaging and advice on thin film characterizations. We acknowledge funding from CFI/ORF LOF to Z.L., which supports AFM infrastructure, including Nanowizard II AFM (JPK).

REFERENCES

(1) Ozaydin-Ince, G.; Coclite, A. M.; Gleason, K. K. *Rep. Prog. Phys.* **2012**, *75*, 016501.
(2) Vendra, V. K.; Wu, L.; Krishnan, S. *Nanostructured Thin Films and Surfaces*; Nanomaterials for the Life Sciences *5*; Wiley-VCH: Weinheim, Germany, 2010, pp 1−54.
(3) Chapman, B. N. *J. Vac. Sci. Technol.* **1974**, *11*, 106−113.
(4) Chen, W.; McCarthy, T. J. *Macromolecules* **1997**, *30*, 78−86.
(5) Gillich, T.; Benetti, E. M.; Rakhmatullina, E.; Konradi, R.; Li, W.; Zhang, A.; Schlüter, A. D.; Textor, M. *J. Am. Chem. Soc.* **2011**, *133*, 10940−10950.
(6) Peterson, I. R. *J. Phys. D: Appl. Phys.* **1990**, *23*, 379−395.
(7) Agarwal, V. K. *Thin Solid Films* **1989**, *179*, 155−160.
(8) Zhou, J.; Ellis, A. V.; Voelcker, N. H. *Electrophoresis* **2010**, *31*, 2−16.
(9) Lee, H.; Dellatore, S. M.; Miller, W. M.; Messersmith, P. B. *Science* **2007**, *318*, 426−430.
(10) Waite, J. H. *Nat. Mater.* **2008**, *7*, 8−9.
(11) Waite, J. H. *Annu. Rev. Mater. Res.* **2011**, *41*, 99−132.
(12) Wise, R. A. *Nat. Rev. Neurosci.* **2004**, *5*, 483−494.
(13) Lee, H.; Scherer, N. F.; Messersmith, P. B. *Proc. Natl. Acad. Sci. U.S.A.* **2006**, *103*, 12999−13003.
(14) Lee, H.; Lee, B. P.; Messersmith, P. B. *Nature* **2007**, *448*, 338−341.
(15) Ball, V.; Frari, D.; Michel, M.; Buehler, M. J.; Toniazzo, V.; Singh, M. K.; Gracio, J.; Ruch, D. *BioNanoScience* **2012**, *2*, 16−34.
(16) Pop-Georgievski, O.; Popelka, T. P. N.; Houska, M.; Chvostov, D.; Proks, V.; Rypacek, F. *Biomacromolecules* **2011**, *12*, 3232−3242.
(17) Ku, S. H.; Lee, J. S.; Park, C. B. *Langmuir* **2010**, *26*, 15104−15108.
(18) Dreyer, D. R.; Miller, D. J.; Freeman, B. D.; Paul, D. R.; Bielawski, C. W. *Langmuir* **2012**, *28*, 6428−6435.
(19) Lee, H.; Rho, J.; Messersmith, P. B. *Adv. Mater.* **2009**, *21*, 431−434.
(20) Kim, S.; Park, C. B. *Langmuir* **2010**, *26*, 14730−14736.
(21) Postma, A.; Yan, Y.; Wang, Y.; Zelikin, A. N.; Tjipto, E.; Caruso, F. *Chem. Mater.* **2009**, *21*, 3042−3044.
(22) Brubaker, C. E.; Messersmith, P. B. *Langmuir* **2012**, *28*, 2200−2205.
(23) Yang, F. K.; Zhao, B. *Open Surf. Sci. J.* **2011**, *3*, 115−122.
(24) Jiang, J. H.; Zhu, L. P.; Zhu, L. J.; Zhu, B. K.; Xu, Y. Y. *Langmuir* **2011**, *27*, 14180−14187.
(25) Yang, F. K.; Zhang, W.; Han, Y.; Yoffe, S.; Cho, Y.; Zhao, B. *Langmuir* **2012**, *28*, 9562−9572.
(26) Jia, M.; Qin, L.; He, X.; Li, W. *J. Mater. Chem.* **2012**, *22*, 707−713.
(27) Chung, H.; Glass, P.; Pothen, J. M.; Sitti, M.; Washburn, N. R. *Biomacromolecules* **2011**, *12*, 342−347.
(28) Johnson, K. L.; Kendall, K.; Roberts, A. D. *Proc. R. Soc. London, Ser. A* **1971**, *324*, 301−313.
(29) Wei, Q.; Zhang, F.; Li, J.; Li, B.; Zhao, C. *Polym. Chem.* **2010**, *1*, 1430−1433.
(30) Shahsavan, H.; Arunbabu, D.; Zhao, B. *Macromol. Mater. Eng.* **2012**, *297*, 743−760.
(31) Rand, C. J.; Crosby, A. J. *J. Appl. Phys.* **2009**, *106*, 064913.
(32) Bernsmann, F.; Ball, V.; Addiego, F.; Ponche, A.; Michel, M.; Gracio, J. J. A.; Toniazzo, V.; Ruch, D. *Langmuir* **2011**, *27*, 2819−2825.
(33) Xie, J.; Michael, P. L.; Zhong, S.; Ma, B.; Macewan, M. R.; Lim, C. T. *J. Biomed. Mater. Res., Part A* **2012**, *100*, 929−938.
(34) Beuth, J. L. *Int. J. Solids Struct.* **1992**, *29*, 1657−1675.
(35) Tsui, T. Y.; McKerrow, A. J.; Vlassak, J. J. *J. Mater. Res.* **2005**, *20*, 2266−2273.
(36) Dundurs, J. *J. Appl. Mech.* **1969**, *36*, 650−652.
(37) Vlassak, J. J. *Int. J. Fract.* **2003**, *119*, 299−323.
(38) Chai, H. *Int. J. Solids Struct.* **2011**, *48*, 1092−1100.
(39) Owens, D. K.; Wendt, R. C. *J. Appl. Polym. Sci.* **1969**, *13*, 1741−1747.
(40) Clint, J. H.; Wicks, A. C. *Int. J. Adhes. Adhes.* **2001**, *21*, 267−273.
(41) Hallab, N. J.; Bundy, K. J.; O'Connor, K.; Moses, R. L.; Jacobs, J. J. *Tissue Eng.* **2001**, *7*, 55−71.
(42) Chen, Y. L.; Helm, C. A.; Israelachvili, J. N. *J. Phys. Chem.* **1991**, *95*, 10736−10747.
(43) Silberzan, P.; Perutz, S.; Kramer, E. J.; Chaudhury, M. K. *Langmuir* **1994**, *10*, 2466−2470.
(44) Liu, X.; Nanao, H.; Li, T.; Mori, S. *Wear* **2004**, *257*, 665−670.
(45) Berman, A.; Drummond, C.; Israelachvili, J. *Tribol. Lett.* **1998**, *4*, 95−101.
(46) Zhang, L.; Shi, J.; Jiang, Z.; Jiang, Y.; Qiao, S.; Li, J.; Wang, R.; Meng, R.; Zhua, Y.; Zheng, Y. *Green Chem.* **2011**, *13*, 300−306.
(47) Bridelli, M. G.; Crippa, P. R. *J. Phys. Chem. B* **2010**, *114*, 9381−9390.
(48) Meredith, P.; Sarna, T. *Pigm. Cell Res.* **2006**, *19*, 572−594.